A&A manuscript no.
(will be inserted by hand later)

Your thesaurus codes are:
02.13.2;08.05.3;08.19.4

ASTRONOMY AND ASTROPHYSICS
December 27, 1999

Nonstationary magnetorotational processes in a rotating magnetized cloud

N.V.Ardeljan[1], G.S.Bisnovatyi-Kogan[2], and S.G.Moiseenko[2]

[1] Department of Computational Mathematics and Cybernetics, Moscow State University, Vorobjevy Gory, Moscow B-234 119899, Russia, ardel@redsun.cs.msu.su
[2] Space Research Institute, Profsoyuznaya 84/32, Moscow 117810, Russia
gkogan@mx.iki.rssi.ru, moiseenko@mx.iki.rssi.ru

Received ; accepted

Abstract. We perform 2D numerical simulations of a magnetorotational explosion of a rotating magnetized gas cloud. We found that amplification of a toroidal magnetic field due to the differential rotation leads to a transformation of the part of the rotational energy of the cloud to the radial kinetic energy. Simulations have been made for 3 initial values of ξ (the relation of magnetic energy to the gravitational energy of the cloud): $\xi = 10^{-2}$, 10^{-4}, 10^{-6}. Part of the matter - $\sim 7\%$ of the mass of the cloud ($\sim 3.3\%$ of the final gravitational energy of the cloud) - gets radial kinetic energy which is larger than its potential energy and can be thrown away to the infinity. It carries about 30% of the initial angular momentum of the cloud. This effect is important for angular momentum loss in the processes of stellar formation, and for the magnetorotational mechanism of explosion suggested for supernovae. Simulations have been made on the basis of the Lagrangian 2D numerical implicit scheme on a triangular grid with grid reconstruction.

Key words: magntohydrodynamics – stars: supernovae – stars: evolution

1. Introduction

Magnetic field plays an important role in life of a star, especially at its birth and its death. A birth of a star in a galactic disk during the collapse of an interstellar cloud is complicated by large angular momentum of matter which will prevent formation of the star if it is not lost. The most realistic mechanism of the angular momentum loss is connected with a magnetic field which, twisting during differential rotation, leads to a flux of angular momentum outside, permiting a collapse of the main body (Bisnovatyi-Kogan et al. 1973, Ardeljan et al. 1996b).

In the late stages of evolution of massive stars, loss of hydrodynamical stability initiates a collapse, which is finished by supernovae explosions after formation of a stable neutron star. Investigation of supernovae explosions in different nonmagnetized models revealed serious problems in transformation of the gravitational energy into the energy of explosion. In this situation magnetorotational mechanism of supernovae explosion, suggested by Bisnovatyi-Kogan (1970) could be an explanation of this phenomena.

Magnetorotational phenomena in stellar envelopes are considered to be a main mechanism of an angular momentum loss from stars, and magnetized solar wind is a reason for a very slow solar rotation.

2D calculations of collapse of a rotating magnetized star with a somewhat unrealistic magnetic field configuration have been performed by Le Blank & Wilson (1970) and Ohnishi (1983). The geometry of the outburst which they obtained, was different, but the energy of the outburst was substantial in both cases.

We investigate here magnetorotational phenomena in the collapsing rotating magnetized gas cloud initially with uniform density and angular momentum, which may be considered as a model of star formation. After magnetorotational explosion a quasistationary, almost uniformly slow rotating configuration is formed. The loss of angular momentum is connected with an outburst of the matter, carrying an energy which is $\sim 3.3\%$ of the final gravitational energy of the cloud. Our simulations show that amounts of ejected mass and energy are weakly dependent on the initial value of magnetic energy (parameter ξ). The main difference in the results of 2D simulations for the different initial values of ξ is in the duration of the process. This conclusion confirms results of 1D simulations (Bisnovatyi-Kogan et al. 1976, Ardeljan et al., 1979), with the time of the process approximately proportional to the $\xi^{-1/2}$. Similar processes related to a different initial model and equation of state are expected to act during supernovae explosions.

Magnetorotational explosion of a rotating magnetized gas cloud in a 2D approach has been investigated earlier by Ardeljan et al. (1996b) for a divergency-free, but not force-free, magnetic field configuration. Magnetic forces

Send offprint requests to: S.G. Moiseenko, moiseenko@mx.iki.rssi.ru

have not been balanced by a pressure distribution and gravitational forces. The effect of ejection of the part of the mass of the cloud has been found there, but use of an unbalanced initial field leads to artificial effects in a MHD flow and does not allow us to extend calculations as far as is needed.

In this paper an initial configuration with magnetic forces balanced by pressure and gravitational forces distribution has been constructed, allowing us to make calculations for different sets of initial parameters and to extend them to the larger times.

2. Basic equations

Consider a set of magnetohydrodynamical equations with selfgravitation and with infinite conductivity (Landau & Lifshitz, 1984, Bisnovatyi-Kogan, 1989):

$$\frac{\mathrm{d}\mathbf{x}}{\mathrm{d}t}=\mathbf{u},\quad \frac{\mathrm{d}\rho}{\mathrm{d}t}+\rho\,\mathrm{div}\,\mathbf{u}=0,$$

$$\rho\frac{\mathrm{d}\mathbf{u}}{\mathrm{d}t}=-\mathrm{grad}\left(p+\frac{\mathbf{H}\cdot\mathbf{H}}{8\pi}\right)+\frac{\mathrm{div}(\mathbf{H}\otimes\mathbf{H})}{4\pi}-\rho\,\mathrm{grad}\,\Phi,$$

$$\rho\frac{\mathrm{d}}{\mathrm{d}t}\left(\frac{\mathbf{H}}{\rho}\right)=\mathbf{H}\cdot\nabla\mathbf{u},\quad \Delta\Phi=4\pi G\rho, \tag{1}$$

$$\rho\frac{\mathrm{d}\varepsilon}{\mathrm{d}t}+p\,\mathrm{div}\,\mathbf{u}=0,\quad \frac{1}{\rho}=\frac{T\Re}{p},\quad \varepsilon=\frac{T\Re}{\gamma-1},$$

where $\frac{\mathrm{d}}{\mathrm{d}t}=\frac{\partial}{\partial t}+\mathbf{u}\cdot\nabla$ is the total time derivative, $\mathbf{x}=(r,\varphi,z)$, $\mathbf{u}$ is velocity vector, ρ is density, p is pressure, $\mathbf{H}=(H_r,\ H_\varphi,\ H_z)$ is magnetic field vector, Φ is gravitational potential, ε is internal energy, G is gravitational constant, $\Re$ is universal gas constant, γ is adiabatic index, $\mathbf{H}\otimes\mathbf{H}$ is tensor of rank 2.

Axial symmetry ($\frac{\partial}{\partial\varphi}$) and symmetry to the equatorial plane ($z=0$) are assumed.

The problem is solved in the restricted domain. Outside the domain, the density of the matter is zero, but poloidal components of magnetic field H_r, H_z can be nonzero.

To write the set of equations in dimensionless form we choose the following scale values:

$$\rho_0=1.492\cdot10^{-17}\mathrm{g/cm}^3,\ r_0=z_0=x_0=3.81\cdot10^{16}\mathrm{cm},$$

$$r=\tilde{r}x_0,\ z=\tilde{z}x_0,\ u=\tilde{u}u_0,\ u_0=\sqrt{4\pi G\rho_0x_0^2},$$

$$p=\tilde{p}p_0,\ \varepsilon=\tilde{\varepsilon}\varepsilon_0,\ T=\tilde{T}T_0,\ \Phi=\tilde{\Phi}\Phi_0,\ \Phi_0=4\pi G\rho_0x_0^2,$$

$$t_0=\frac{x_0}{u_0},\ p_0=\rho_0u_0^2=\rho_0x_0^2t_0^{-2},\ T_0=\frac{u_0^2}{\Re},$$

$$\varepsilon_0=u_0^2=x_0^2t_0^{-2},\ H_0=\sqrt{p_0}=x_0t_0^{-1}\rho_0^{1/2}.$$

Here the values with index zero are the scale factors and the functions under a tilde are dimensionless functions. The set of equations (1) can be written in the following nondimentional form (the tilde being omitted):

$$\frac{\mathrm{d}\mathbf{x}}{\mathrm{d}t}=\mathbf{u},\quad \frac{\mathrm{d}\rho}{\mathrm{d}t}+\rho\,\mathrm{div}\,\mathbf{u}=0,$$

$$\rho\frac{\mathrm{d}\mathbf{u}}{\mathrm{d}t}=-\mathrm{grad}\left(p+\frac{\mathbf{H}\cdot\mathbf{H}}{8\pi}\right)+\frac{\mathrm{div}(\mathbf{H}\otimes\mathbf{H})}{4\pi}-\rho\,\mathrm{grad}\,\Phi,$$

$$\rho\frac{\mathrm{d}}{\mathrm{d}t}\left(\frac{\mathbf{H}}{\rho}\right)=\mathbf{H}\cdot\nabla\mathbf{u},\quad \Delta\Phi=\rho, \tag{2}$$

$$\rho\frac{\mathrm{d}\varepsilon}{\mathrm{d}t}+p\,\mathrm{div}\,\mathbf{u}=0,\quad \frac{1}{\rho}=\frac{T}{p},\quad \varepsilon=\frac{T}{\gamma-1}.$$

Taking into account symmetry assumptions ($\frac{\partial}{\partial\varphi}=0$), the divergency of the tensor $\mathbf{H}\otimes\mathbf{H}$ can be presented in the following form:

$$\mathrm{div}(\mathbf{H}\otimes\mathbf{H})=\begin{pmatrix}\frac{1}{r}\frac{\partial(rH_rH_r)}{\partial r}+\frac{\partial(H_zH_r)}{\partial z}-\frac{1}{r}H_\varphi H_\varphi\\ \frac{1}{r}\frac{\partial(rH_rH_\varphi)}{\partial r}+\frac{\partial(H_zH_\varphi)}{\partial z}+\frac{1}{r}H_\varphi H_r\\ \frac{1}{r}\frac{\partial(rH_rH_z)}{\partial r}+\frac{\partial(H_zH_z)}{\partial z}\end{pmatrix}.$$

3. Collapse of a rotating magnetized gas cloud

3.1. Formulation of the problem

Consider a magnetized rotating gas cloud which is described by the set of equations (1). All graphs and figures below are in a nondimensional form. At the initial moment ($t=0$) the cloud is a rigidly rotating uniform gas sphere (Fig. 1) with the following parameters:

$$r=3.81\cdot10^{16}\mathrm{cm},\ \rho=1.492\cdot10^{-17}\mathrm{g/cm}^3,\ \eta=5/3,$$

$$M=1.73M_\odot=3.457\cdot10^{33}\mathrm{g},\ u^r=u^z=0, \tag{3}$$

$$\beta_{r0}=\frac{E_{\mathrm{rot}0}}{|E_{\mathrm{gr}0}|}=0.04, \tag{4}$$

$$\beta_{i0}=\frac{E_{\mathrm{in}0}}{|E_{\mathrm{gr}0}|}=0.01, \tag{5}$$

$$\xi=\frac{E_{\mathrm{magl}}}{|E_{\mathrm{gr}1}|}=10^{-2},\ 10^{-4},10^{-6}. \tag{6}$$

Here the subscript "0" corresponds to the initial moment ($t=0$), subscript "1" to the moment of the beginning of the evolution of magnetic field ($t=t_1>0$).

The assumptions about the symmetry of the problem are the same as in Section 2.

The process can be divided into the following three qualitatively different stages. First is a pretty short hydrodynamical collapse stage. At this stage the influence of the magnetic field on the process of the collapse of the

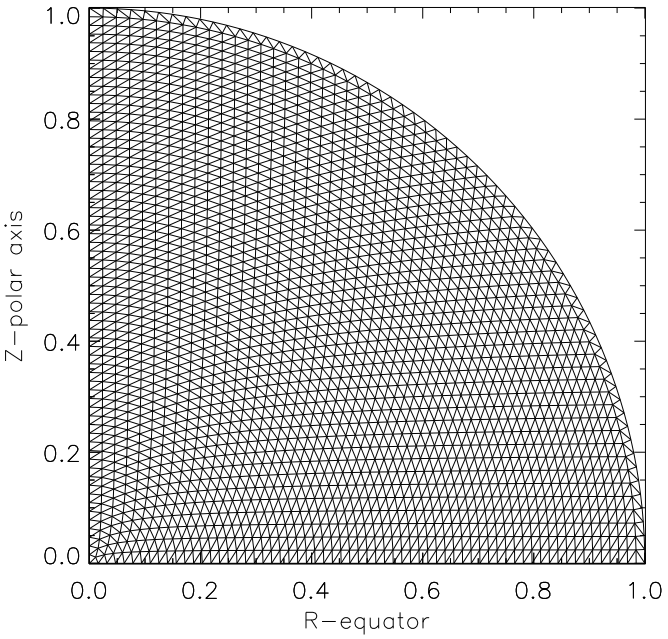

Fig. 1. Grid at initial time $t = 0$.

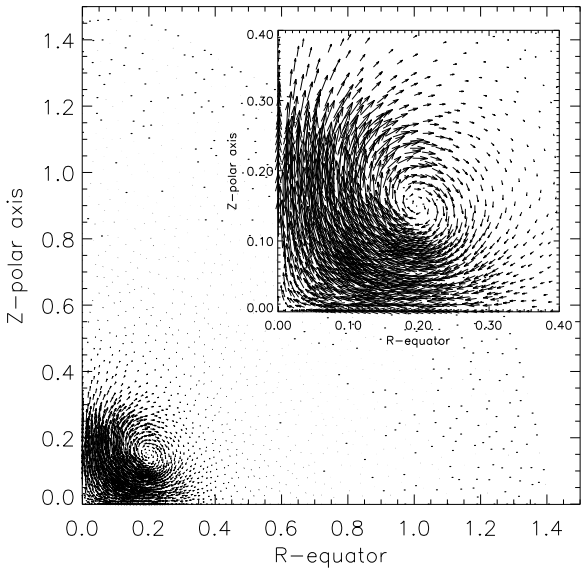

Fig. 2. Initial magnetic field, produced by current (7). Upper right part of the figure is the magnetic field in the central part of the cloud.

cloud can be neglected, because the initial poloidal magnetic field is weak. In the short time of collapse the toroidal component of the magnetic field, which appears to be due to the arising differential rotation is also weak at this initial stage. The second stage is the stage of a rather "long" twisting of magnetic field due to the differential rotation of the cloud. The final third stage starts with the appearance of a compression wave, moving from the inner parts of the cloud to its periphery along a steeply decreasing density background. Soon after its appearance, it transforms into the MHD shock wave, which can push out a light envelope of the protostar. Similar ejection following formation of a rapidly rotating neutron star and a differentially rotating envelope, can be interpreted as supernova explosion.

Simulations for different ξ consist of the calculation of oscillations of the cloud until formation of the differentially rotating equilibrium (without magnetic field), and subsequent inclusion and twisting of the magnetic field.

3.2. Initial magnetic field configuration

The initial magnetic field must satisfy the condition of absence of magnetic charges div$\mathbf{H} = 0$. It also has to correspond to the boundary conditions of the problem.

The best choice would be dipole or quadrupole. While they satisfy initial and boundary conditions, they have singularities in the origin of coordinates ($r = 0$, $z = 0$). Using such magnetic fields in numerical simulations can lead to loss of accuracy of calculations.

To define the initial magnetic field we use the following method. We defined toroidal current j_φ in the central part of the core of the collapsed cloud by a formula:

$$
\begin{aligned}
j_\varphi &= j^u_\varphi + j^d_\varphi, \qquad (7)\\
j^u_\varphi &= \left[\sin\left(\pi\frac{r}{0.3}-\frac{\pi}{2}\right)+1\right]\left[\sin\left(\pi\frac{z}{0.3}-\frac{\pi}{2}\right)+1\right]\\
&\quad\times\left[1-\left(\frac{r}{0.3}\right)^2-\left(\frac{z}{0.3}\right)^2\right],\\
&\quad \text{at } r^2+z^2<0.3^2,\ z>0,\\
j^d_\varphi &= -j^u_\varphi \text{ at } r^2+z^2<0.3^2,\ z<0.
\end{aligned}
$$

After getting the defferentially rotating stationary solution for nonmagnetized cloud we use Bio-Savara law (A1),(A2),(A5) for calculation of the poloidal components of the magnetic field H_{r0}, H_{z0} (Fig. 2). This magnetic field is divergency free, but it is not force-free and should be balanced at the initial moment. Then we use the following method: we "turn on" the poloidal magnetic field H_{r0}, H_{z0}, but "switch off" the equation for the evolution of the toroidal component H_φ in (1). Actually it means that we define $H_\varphi \equiv 0$, $\frac{\mathrm{d}H_\varphi}{\mathrm{d}t} \equiv 0$. From the physical point of view it means that we allow magnetic field lines to slip through the matter of the cloud in the toroidal direction. After "turning on " such a field, we let the cloud come to the steady state, where magnetic forces connected with the purely poloidal field are balanced by other forces.

The calculated balanced configuration has the magnetic field of quadrupole-like symmetry. For testing we run our code with this purely poloidal field for a large number of time steps ($\sim 10^3$), during which the parameters of the cloud did not change.

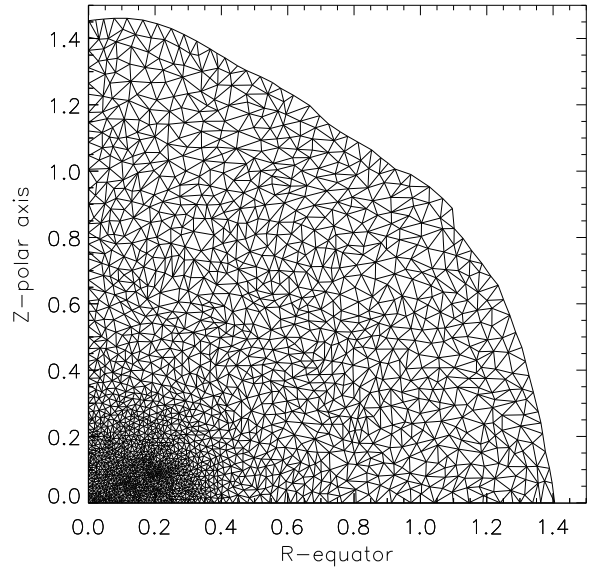

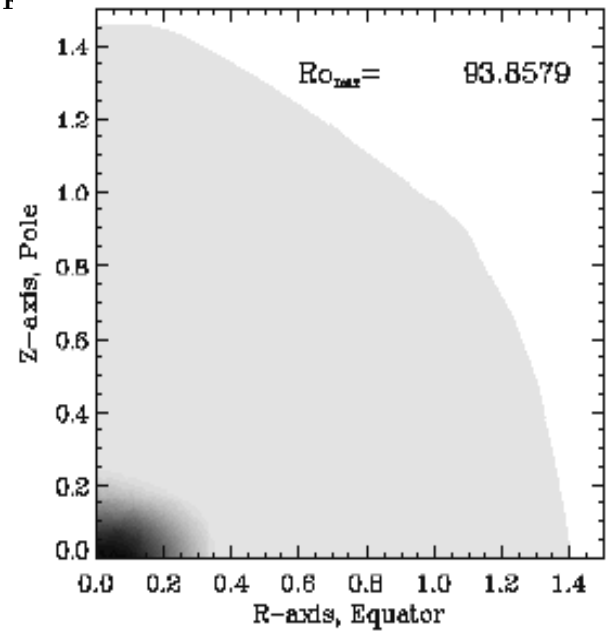

Fig. 4. Density field at $t_1 = 18.45$.

4. Results

We describe results of simulations of the problem for initial $\xi(t_1) = 10^{-2}$. Results of simulations for $\xi(t_1) = 10^{-4}, 10^{-6}$ are qualitatively similar to the first case. The amounts of the ejected mass and energy are the same, $\sim 7\%$ of mass and $\sim 3.3\%$ of energy. The main difference betveen these three variants is the duration of the process. The lower the initial magnetic energy, the longer the evolution time up to the magnetorotational explosion. This feature of the results of the simulations in a 2D case is similar to the results of 1D simulations of the magnetorotational mechanism for supernovae (Ardeljan, et.al. 1979).

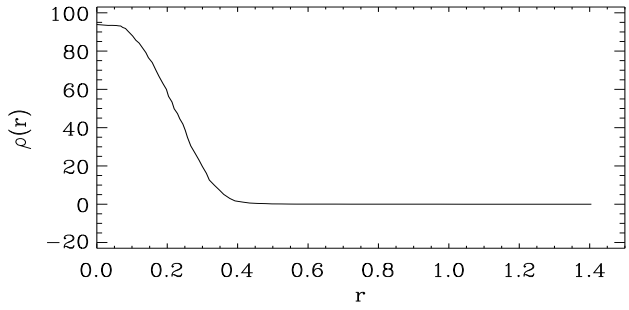

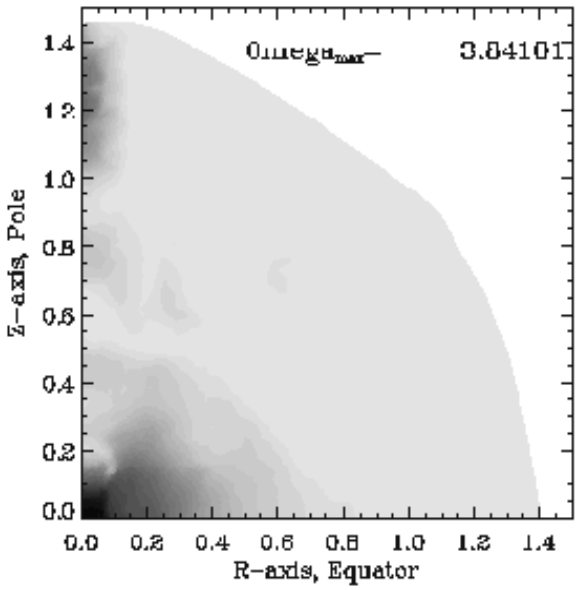

Fig. 6. Angular velocity levels at $t_1 = 18.45$.

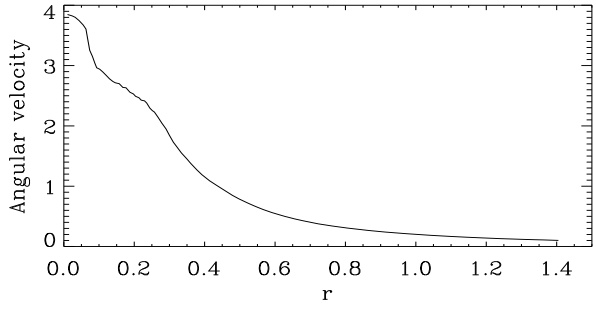

Fig. 7. Angular velocity distribution along r axis at $t_1 = 18.45$.

We start calculations ($t = 0$) with the set of initial parameters (3)–(5) (without magnetic field at the beginning). Our triangular grid at $t = 0$ consists of 2200 knots and 4400 cells. During the calculations, the number of knots and cells deviates no more than 5% from its initial values due to specially developed procedure (Ardeljan, et.al. 1996a). After a number of oscillations the cloud at $t_1 = 18.45$ comes to the steady differentially rotating

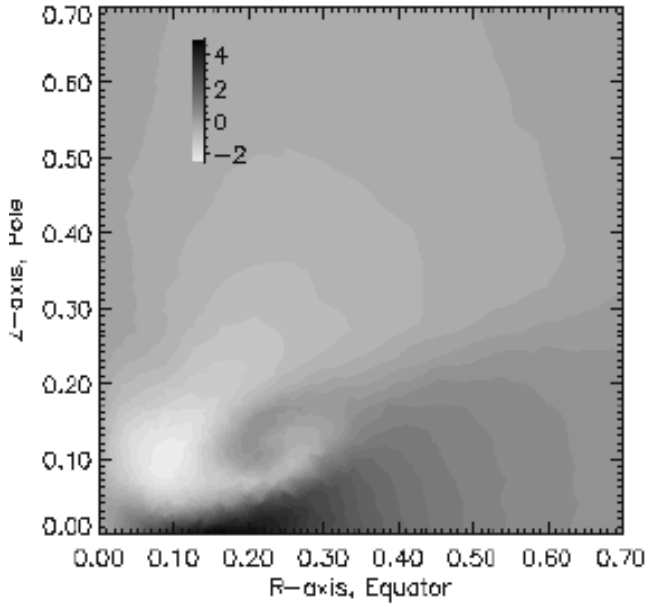

Fig. 8. Toroidal magnetic field at $t = 28.35$.

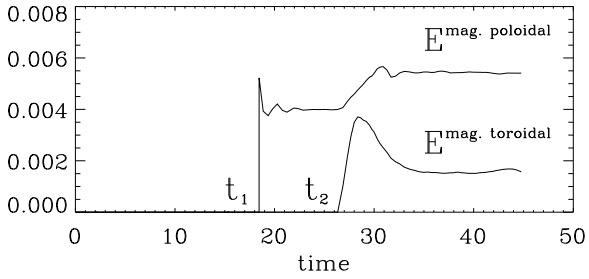

Fig. 9. Time evolution of poloidal and toroidal magnetic energies. t_1 is the moment of turning on the initial poloidal magnetic field, t_2 is the moment of the beginning of the evolution of the toroidal magnetic field.

configuration. Lagrangian grid, density field and angular velocity levels are shown in Figs. 3, 4, 6. Distribution of the density and angular velocity for the $t_1 = 18.45$ along r-axis are given in Figs. 5, 7.

At t_1 the cloud consists of a rapidly rotating dense core and a slowly rotating prolate envelope (Figs. 5, 7). The radial part of kinetic energy of the cloud is less than 1.5% of its gravitational energy. The cloud can stay an infinite time in such differentially rotating stationary condition (if we neglect dissipation processes). However inclusion of even a weak magnetic field leads to an essential change in its state.

At t_1 we "turn on" a poloidal magnetic field calculated as described above. Simultaneously at t_1 we "switch off" the equation for the evolution of the toroidal magnetic field H_φ for a short time (as discussed in the section "Initial magnetic field configuration"). After a few weak oscillations around equilibrium, the cloud comes to the steady state configuration with a balanced magnetic force. These

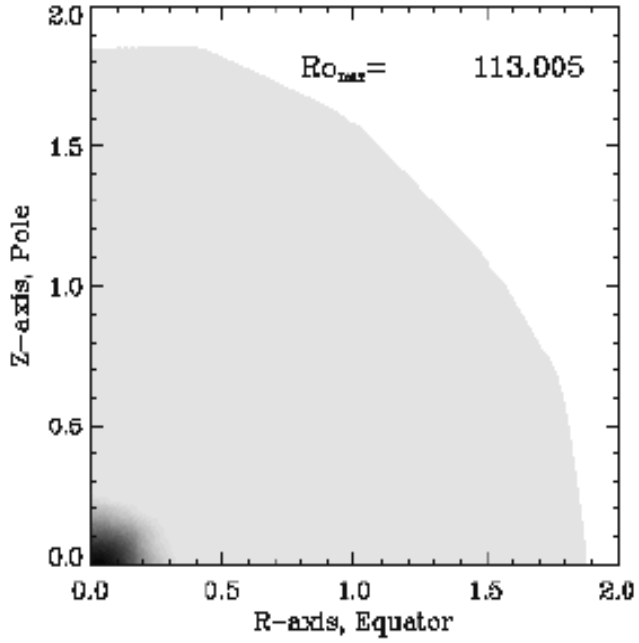

Fig. 10. Density distribution at $t = 28.0$, beginning the evolution of the toroidal magnetic field. The black colour corresponds to the maximal density.

oscillations are clearly seen in the plot for the time evolution of the poloidal magnetic energy (Fig. 9) This purely poloidal field becomes balanced at $t_2 = 26.86$. At this time we "switch on" the equation for the toroidal component of magnetic field and let the magnetic force lines twist due to differential rotation.

Due to the differential rotation of the cloud and very high (infinite) conductivity soon after $t = t_2$, the toroidal component of magnetic field appears and grows with time. Taking into account the quadrupole-like symmetry of the initial poloidal magnetic fields the toroidal component appears and has 2 extremes (Fig. 8). A maximum at the equatorial plane and a minimum at the periphery of the core of the cloud, close to the z-axis. These extrema at the initial stage of the evolution of the toroidal magnetic field correspond approximately to the extremes of the following scalar product: $\mathbf{H} \cdot \mathrm{grad}\frac{V_\varphi}{r}$, because the cloud at the moment of "switching on" the equation for toroidal magnetic field was in a steady state condition and only this term in the equation for the H_φ determines the evolution of the toroidal field.

Toroidal magnetic energy grows almost linearly starting from t_2 up to reaching its maximum value (Fig. 9) after ~ 2.5 rotations of the central core, which rotates almost rigidly. Increase of the toroidal magnetic field leads to subtraction of angular momentum from the central parts of the cloud and additional contraction of the core of the cloud, meanwhile the envelope of the cloud starts to blow up. Contraction wave moving outwards appears at the periphery of the core of the cloud. This wave propagates

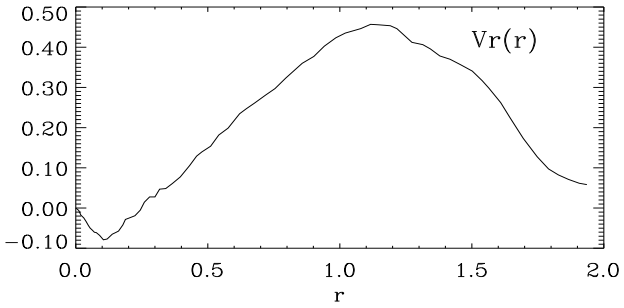

Fig. 11. Radial velocity v_r distribution along the r axis at $t_1 = 28.886$.

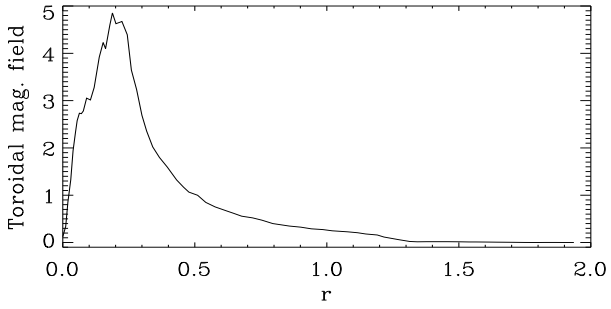

Fig. 12. Toroidal magnetic field H_φ distribution along the r axis at $t_1 = 28.886$.

along a decreasing density profile, increasing its amplitude and transforms to the MHD shock wave.

At $t = 28.0$ a small outer part of the envelope of the cloud reaches the poloidal (radial) velocity (v_r, v_z), which corresponds to a kinetic energy larger then its potential energy and can fly away to infinity. At this time maximal density in the center of the cloud is $\rho_{max} = 113.0$ (Fig. 10). The amount of matter thrown away by the MHD shock, grows with time. In figs.14,15 one can see the evolution of the velocity field and development of the process of ejection of the matter of the envelope of the cloud with time.

The growth of the toroidal magnetic field leads to the formation of MHD shocks. To analyze the structure of the evolution of these shocks we consider a flow picture at the equatorial plane (along r-axis). The toroidal field at the r-axis, has the maximum at the periphery of the core of the cloud, approximately coinciding with the point where the radial velocity v_r changes its sign (Fig. 11). At $r \approx 0.15$ (Fig. 13) MHD shock is formed, and it is a slow MHD shock, because its velocity is lower than the local Alfvenic velocity. Angular velocity v_φ/r and H_φ is decreasing, when passing through this shock. The density ρ and temperature T are increasing.

The matter which is on the right part of the maximum of H_φ is moving outwards. The MHD shock, which is formed on the right side of the maximum of the

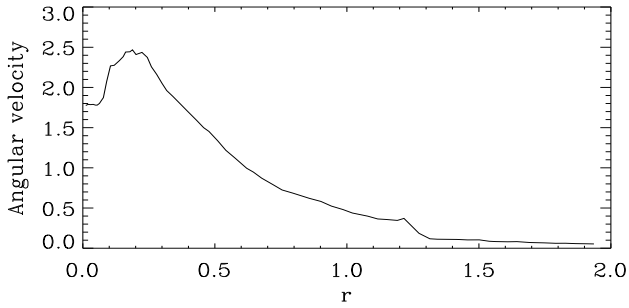

Fig. 13. Angular velocity V_φ/r distribution along the r axis at $t_1 = 28.886$.

toroidal field at the equatorial plane is a fast MHD shock wave, and its velocity is bigger than fast magnetic sound speed before the front of the shock. The velocity of the MHD shock wave is smaller than the Alfvenic sound speed in the gas behind the shock, and bigger than the slow magnetic sound speed after the shock Kulikovskii & Ljubimov, 1962. The toroidal magnetic field (Fig. 12) and angular velocity (Fig. 13) grow behind the shock. Due to the transformation of the rotational energy into the kinetic energy of the radial motion, the angular velocity of the core of the cloud decreases with time (Fig.13). At $t = 28.886$ the shock is at $r \approx 1.25$ (see for example Fig.13).

Similar slow MHD shock has been found in 1D simulations of magnetrotational supernova explosion made by Ardeljan, et.al. (1979), while the formation of the fast MHD shock was not presented.

The time evolution of the parameters

$$\beta_r(t) = \frac{E_{\rm rot}(t)}{|E_{\rm gr}(t)|},\ \beta_i(t) = \frac{E_{\rm in}(t)}{|E_{\rm gr}(t)|},\ \xi(t) = \frac{E_{\rm mag}(t)}{|E_{\rm gr}(t)|}, \qquad (8)$$

for initial $\xi(t_1) = 10^{-2}$, is given in Fig.(16).

In Figs. 17 and 18, time evolution is presented of the ejected mass of the envelope of the cloud, and the energy it carries away. Just after the beginning of the ejection the amount of the ejected mass grows approximately linearly with time. At the moment $t = 33.57$, its growth stops and until the end of the calculations these values (ejected mass and energy) do not change significantly. The amount of the ejected matter after this time is about 7% and it carries approximately 3.3% of the total energy of the cloud. At the moment of the evolution of the magnetorotational explosion the rotation of the cloud changes essentially. The core of the cloud now rotates with the small angular velocity $\omega_{core} \approx 0.85$. The ejecting matter now looks like an expanding shell. At $t = 28.0$ (the moment of the "switching on" of the evolution of the toroidal magnetic field, the "inner" (core and part of the envelope) 50% of the mass of the cloud contained 26.8% of the angular momentum, at $t = 33.57$ the "inner" 50% of the mass of the cloud contained 7.2% of the angular momentum. At $t = 28.0$ the

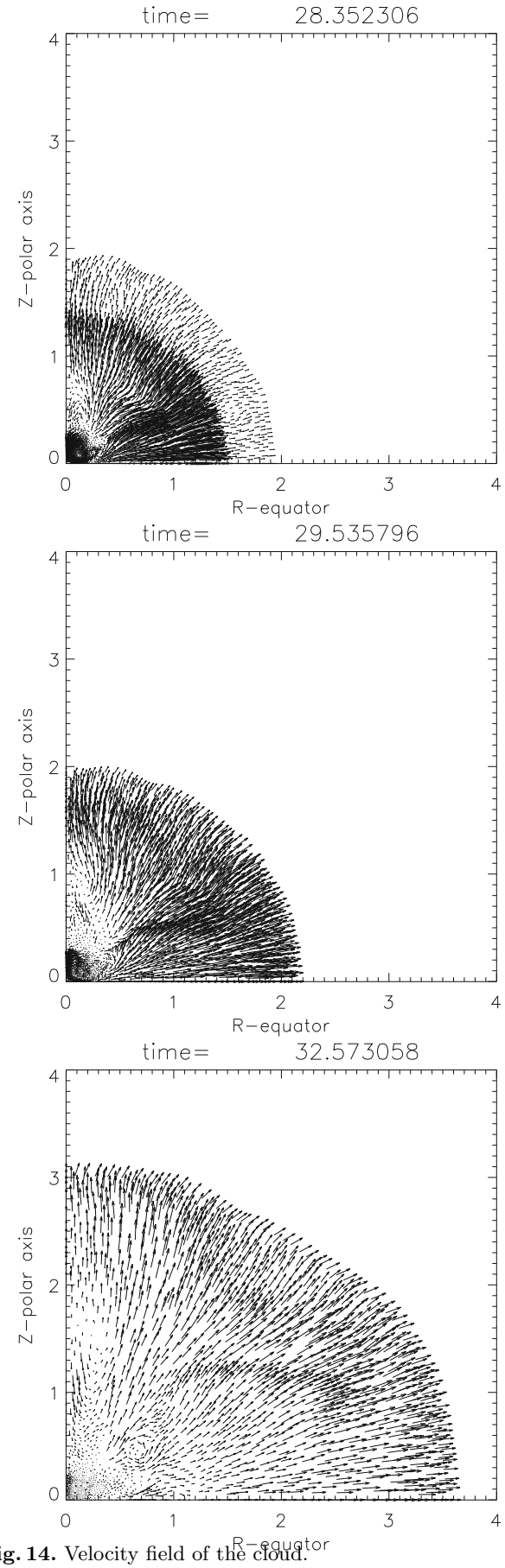

Fig. 14. Velocity field of the cloud.

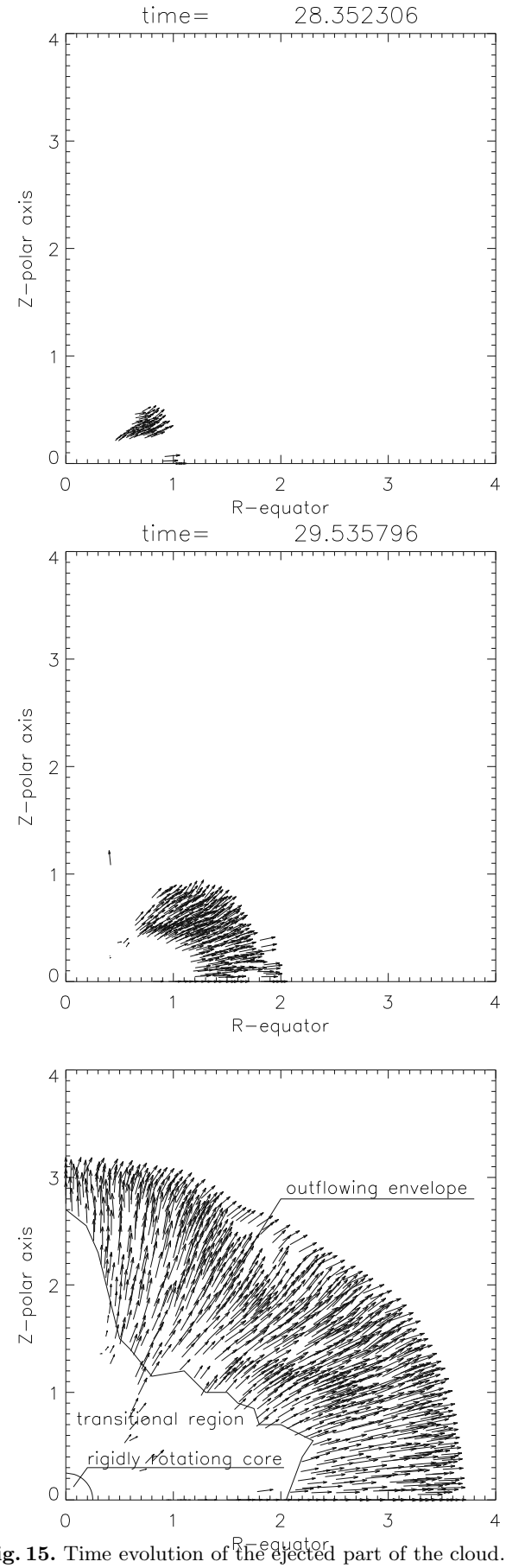

Fig. 15. Time evolution of the ejected part of the cloud.

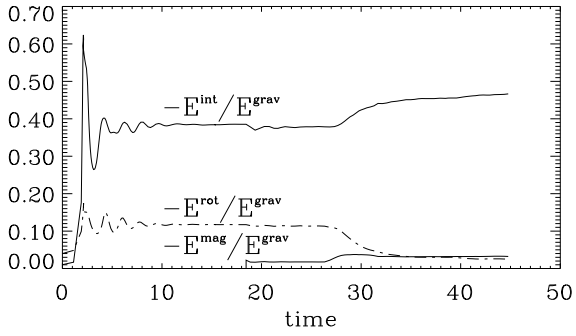

Fig. 16. Time evolution of parameters ξ, β_i, β_r. for $\xi(t_1) = 10^{-2}$

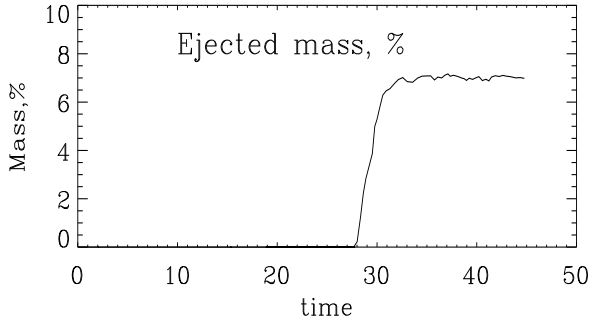

Fig. 17. Time evolution (in %) of the ejected mass of the envelope of the cloud.

50% of the angular momentum are contained in the outer part of the envelope of the cloud (31.3% of the mass of the cloud). At $t = 33.57$ the 50% of the angular momentum is concentrated in the outer part of the envelope of the cloud (9.2% of the mass of the cloud). At the last plot of Fig. 15 the structure of the cloud at the advanced stage of the magnetorotational explosion is given. At this stage the cloud consists of an outflowing envelope, a transitional region and an almost rigidly rotating core.

In the paper by Ardeljan et al., 1979 it was found in 1D calculations of the magnetorotational supernova explosion that during the evolution of the toroidal component and angular momentum transfer outwards, the central core of the cloud starts to rotate in the opposite direction to the initial one. Such magnetorotational oscillations have been investigated analytically by Bisnovatyi-Kogan et al. 1976. With respect to the star formation problems in slightly different formulation, these oscillations have been investigated in the papers by Moushovias & Paleologou, 1979, Moushovias & Paleologou, 1980. In our simulations we do not get the opposite rotation of the core of the cloud in the opposite direction. However the core loses significant part of its angular momentum due to magnetic breaking.

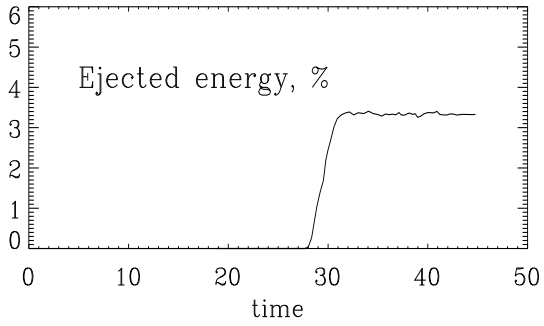

Fig. 18. Time evolution (in % to the total initial energy of the cloud) of the energy of the ejected matter of the envelope of the cloud.

5. Discussion

The first 2D calculations of the magnetorotational explosion were performed by Le Blank & Wilson (1970), where matter was expelled in the form of jets. Such geometry of the outburst was the result of a specific rather unrealistic choice of the magnetic field configuration, which was produced by a current ring, at an equator, out of a stellar centre, where the matter density was an order of magnitude less than a central one. The magnetic field of this ring had a zero radial component in the equatorial plane, and a magnetic pressure gradient was formed in the z-direction due to the differential rotation, which almost repeated the magnetic pressure gradient of the initial configuration. Such magnetic field structure had led to the matter stream pattern appearing preferentially along the symmetry axis of the magnetic field.

In our calculations the magnetic field was created by the oppositely directed current rings in the central region of the star. The magnetic field had a quadrupole-like configuration with a maximum value close to the centre of the star, and large radial component at the equator.

In the papers devoted to the simulations of the star formation problems (e.g. Ciolek & Mouschovias, 1995; Tomisaka, 1998) it is often supposed that the initial poloidal magnetic field has only an H_z component. It is often suggested for the collapse problem of protostellar clouds. We should point out that the initial magnetic field of the configuration $H_{0z} \neq 0$, $H_{0r} = 0$ or dipole-like magnetic fields ($H_{0r} = 0$ at the equatorial plane) can lead after, the evolution of the toroidal component, to the jet-like outflows directed presumably along the z-axis. However application of the quadrupole-like initial poloidal field ($H_z = 0$ at the equatorial plane) can give radial ejections, as is seen in our results.

The initial magnetic field configuration in the rotating gas cloud as a progenitor of the star formation may be rather complicated because of noncoincidence of magnetic and rotational axes and possible action of the dynamo mechanism. Due to this fact the prevailing of a

quadrupole-like component in the initial model it seems to be possible in some cases also in the cloud.

Observation of the solar corona during sunspot minimum has shown a north-south asymmetry, interpreted by Osherovich et al. (1984) as the presence of a significant magnetic quadrupole. Due to more rapid central increase of the quadrupole component ($\sim 1/r^4$) in comparison with the dipole ($\sim 1/r^3$), we may expect that quadrupole component may be larger than the dipole one in the central part of the star. Besides, we believe that the maximum of the magnetic field strength can not be situated at such large distance from the centre, as it was taken by Le Blank & Wilson (1970). Another 2D calculation, performed by Ohnishi (1983) for a radial initial magnetic field gave an outburst mainly in the equatorial plane, similar to our results.

The amount of energy of the matter ejected during the magnetorotational explosion is sufficient for producing a supernova explosion after formation of the rapidly rotating neutron star with a differentially rotating envelope. Such calculations are now in progress.

Appendix A: Numerical method

We have used a numerical technique, based on a conservative (in the absence of gravitation), implicit first order of accuracy in space and time operator difference scheme on a triangular grid with a grid reconstruction, developed and described in Ardeljan et al. (1987), Ardeljan & Kosmachevskii (1995). This numerical method has been used in the paper by Ardeljan et al. (1996a) for the investigation of the collapse of the nonmagnetized rotating cloud.

For a numerical solution of the problem of the magnetorotational explosion, we introduce a triangular grid, covering the restricted domain in r, z coordinates.

We suppose that components of the velocity vector $\mathbf{u}$ and gravitational potential Φ will be defined in all knots of the grid. The density ρ, pressure p, components of magnetic field vector $\mathbf{H}$ will be defined in the cells and in the boundary knots of the grid.

For the numerical simulation of the system of gravitational MHD equations the following method has been used. Instead of differential operators (div, grad, rot) we introduce their finite difference analogues. On the base of such operators a completely conservative scheme has been constructed. The scheme is implicit for all velocity components v_r, v_φ, v_z and for the toroidal component of the magnetic field H_φ. The scheme is explicit for the poloidal magnetic field H_r, H_z. The explicitness of the scheme for H_r, H_z does not introduce strong restriction on the time step, because during the evolution of the magnetic field its poloidal values do not change strongly, while the toroidal component appears and increases significantly with time. The scheme is explicit for the gravitational potential, but it was shown in Ardeljan et al. (1987) that this explicitness does not introduce significant restrictions on the time step.

A.1. Calculation of the initial and boundary values of the magnetic field

Initial values of the poloidal components of the magnetic field H_{r_0}, H_{z_0} in the computational domain and its boundary values at the outer boundary H_{rq}, H_{zq} are calculated using the Bio-Savara law:

$$\mathbf{H}(M_0) = \frac{1}{c}\int\limits_V \frac{\mathbf{J}\times\mathbf{R}_{MM_0}}{{R_{MM_0}}^3} dV_M, \tag{A1}$$

where $\mathbf{J} = j_r\mathbf{e}_r + j_\varphi\mathbf{e}_\varphi + j_z\mathbf{e}_z$ - current density, $\mathbf{e}_r, \mathbf{e}_\varphi, \mathbf{e}_z$ - unit vectors of cylindrical system of coordinates, c - light velocity, $\mathbf{R}_{MM_0}$ - radius vector connecting M_0 and M points, R_{MM_0} - length of the vector $\mathbf{R}_{MM_0}$.

In the cylindrical coordinates we have:

$$\mathbf{H}(M_0) = \frac{1}{c}\int\limits_S rds\left(\int\limits_0^{2\pi} \frac{\mathbf{J}\times\mathbf{R}_{MM_0}}{{R_{MM_0}}^3} d\varphi\right). \tag{A2}$$

where S is the computational domain in r, z coordinates.

On the triangular grid the integral $\int\limits_S f(r,z)rds$ can be approximated by the following sum:

$$\int\limits_S f(r,z)rds \approx \sum_{\triangle\in\omega_i} r_i s_i f(r_i, z_i) \tag{A3}$$

where ω_i is a set of triangular cells, r_i is r coordinate of the center of the cell i, z_i is z coordinate of the center of the cell i, s_i – area of the grid cell i.

For the integration of the vector-function in cylindrical coordinates we use the following formula:

$$\int\limits_{\varphi_1}^{\varphi_2}\Big[f_r(\varphi)\mathbf{e}_r + f_\varphi(\varphi)\mathbf{e}_\varphi + f_z(\varphi)\mathbf{e}_z\Big]d\varphi$$

$$= \mathbf{e}_r(\varphi_2)\int\limits_{\varphi_1}^{\varphi_2}\Big[f_r(\varphi)\cos(\varphi_2-\varphi) + f_\varphi(\varphi)\sin(\varphi_2-\varphi)\Big]d\varphi$$

$$+\mathbf{e}_\varphi(\varphi_2)\int\limits_{\varphi_1}^{\varphi_2}\Big[f_\varphi(\varphi)\cos(\varphi_2-\varphi) - f_r(\varphi)\sin(\varphi_2-\varphi)\Big]d\varphi$$

$$+\mathbf{e}_z(\varphi_2)\int\limits_{\varphi_1}^{\varphi_2} f_z(\varphi)d\varphi. \tag{A4}$$

Using (A4) for (A2), after transformations we get:

$$H_r(r,z)=\sum_{\triangle_i\in\omega_i} r_i s_i j_{\varphi i}\Bigg\{$$

$$(z-z_i)\frac{4}{a_1^3}\left[\frac{2-k_1^2}{k_1^2}\Pi\big(-k_1^2,k_1,\frac{\pi}{2}\big)-\frac{2}{k_1^2}F\big(k_1,\frac{\pi}{2}\big)\right]$$

$$+(z+z_i)\frac{4}{a_2^3}\left[\frac{2-k_2^2}{k_2^2}\Pi\big(-k_2^2,k_2,\frac{\pi}{2}\big)-\frac{2}{k_2^2}F\big(k_2,\frac{\pi}{2}\big)\right]\Bigg\},$$

$$H_\varphi(r,z)=0, \tag{A5}$$

$$H_z(r,z)=\sum_{\triangle_i\in\omega_i} r_i s_i j_{\varphi i}\Bigg\{r_i\frac{4}{a_1^3}\Pi\big(-k_1^2,k_1,\frac{\pi}{2}\big)$$

$$+r\frac{4}{a_1^3}\left[\frac{2-k_1^2}{k_1^2}\Pi\big(-k_1^2,k_1,\frac{\pi}{2}\big)-\frac{2}{k_1^2}F\big(k_1,\frac{\pi}{2}\big)\right]$$

$$+r_i\frac{4}{a_2^3}\Pi\big(-k_2^2,k_2,\frac{\pi}{2}\big)$$

$$-r\frac{4}{a_2^3}\left[\frac{2-k_2^2}{k_2^2}\Pi\big(-k_2^2,k_2,\frac{\pi}{2}\big)-\frac{2}{k_2^2}F\big(k_2,\frac{\pi}{2}\big)\right]\Bigg\}.$$

Here

$${k_1}^2=\frac{4r_i r}{{a_1}^2},\ {a_1}^2=(r_i+r)^2+(z-z_i)^2,$$
$${k_2}^2=\frac{4r_i r}{{a_2}^2},\ {a_2}^2=(r_i+r)^2+(z+z_i)^2,$$

$j_{\varphi i}$ is the toroidal component of the current in the center of the cell i,

$F(k,\frac{\pi}{2})=\int\limits_0^{\pi/2}\frac{dt}{\sqrt{(1-k^2\sin^2 t)}}$ – elliptic integral of the first kind,

$\Pi(-k^2,k,\frac{\pi}{2})=\int\limits_0^{\pi/2}\frac{dt}{(1-k^2\sin^2 t)^{3/2}}$ – elliptic integral of the third kind.

Taking into account, that $\mathbf{J}=\frac{c}{4\pi}\mathrm{rot}\mathbf{H}$, and using (A5) we get boundary values of the poloidal magnetic field at the outer boundary.

Approximation error for boundary values of the poloidal components of the magnetic field in the formulae (A5) is $O(h)$. However using these formulae requires $O(N\sqrt{N})$ operations (where N is the total number of grid knots) and takes a lot of CPU time. During calculation the values of the poloidal components of magnetic field at the outer boundary change weakly and to decrease CPU time we used formula (A5) every tenth time step. At all other time steps we extrapolate poloidal fields from the vicinity of the outer boundary to the outer boundary.

A.2. Testing

Testing of the numerical technique, applied in this paper, without magnetic field has been described in detail by Ardeljan et al. (1996a).

In MHD case we add the following tests:

1. We calculated a spherically symmetrical collapse of a nonrotating gas cloud without a magnetic field until the cloud comes to the steady state condition. After that we "turned on" force-free and divergency-free magnetic field $H_r=0$, $H_\varphi=0$, $H_z=\mathrm{const}$. This magnetic field does not change the condition of the cloud after hundreds of numerical time steps.
2. *The piston problem.*[1] Consider the flat piston, which is pushed along the r-axis (our domain for this test was a rectangle with the following coordinates: ($r_0=1000$, $z_0=0$; $r_1=1001$, $z_1=1$), in this case we can consider r, z as Cartesian coordinates with high accuracy) into the gas with following characteristics: infinite conductivity ($\sigma=\infty$), equation of state:

$$p=\Re\rho T,\ \varepsilon=\Re T/(\gamma-1),\ \Re=1,\ \gamma=5/3.$$

At $t=0$ the gas has the following parameters:

$$u_{r0}=0,\ u_{z0}=0,\ \rho_0=1,\ T_0=0,$$

$$H_{r0}=2.507,\ H_{z0}=1.401.$$

The piston has a velocity:

$$v_{r\ \mathrm{piston}}=0.25,\ v_{z\ \mathrm{piston}}=-0.2735.$$

The values of the parameters of the gas after the shock wave front (defined by the Hugoniot formulae) are the following:

$$u_r=0.25,\ u_z=-0.2735,\ T=0.0117,\ \rho=1.33,$$

$$H_r=2.507,\ H_z=2.802.$$

The discrepancy in the analytical and numerical values after the MHD shock was $<1\%$ for the magnetic field and $<0.5\%$ for the density. The same test has been made for the shock, moving along z-axis with similar discrepancy.

Acknowledgements. S.G.M. and G.S.B.-K. are grateful for the partial support to RFBR by grant 99-02-18180, grant of the Russian ministry of science "Astronomy program" No. 1.2.6.5. N.V.A. is thankful for the partial support to the Russian ministry of education, program "Universities of Russia - fundamental researches".

[1] The numerical data, used in this test are taken from Samarskii & Popov (1992)

References

Ardeljan, N.V, Bisnovatyi-Kogan, G.S., Popov , Ju.P. 1979, Aston.Zh., 56, 1244

Ardeljan, N.V, Kosmachevskii, K.V., Chernigovskii, S.V., 1987, Problems of construction and research of conservative difference schemes for magneto-gas-dynamics, MSU, Moscow (in Russian)

Ardeljan, N.V,, Bisnovatyi-Kogan, G.S., Kosmachevskii, K.V., Moiseenko, S.G. 1996a, A&AS, 115, 573

Ardeljan, N.V,, Bisnovatyi-Kogan, G.S., Moiseenko, S.G. 1996b, ApSS, 239, 1

Ardeljan, N.V,, Kosmachevskii, K.V. 1995, Computational mathematics and modeling, 6, 209

Bisnovatyi-Kogan, G.S. 1970, Astron. Zh., 47, 813; 1971,Sov. Astron., 14, 652

Bisnovatyi-Kogan, G.S. 1989, Physical problems of stellar evolution, Nauka, Moscow (in Russian)

Bisnovatyi-Kogan, G.S., Popov, Ju.P. and Samokhin, A.A. 1976 ApSS, 41, 287.

Bisnovatyi-Kogan, G.S., Ruzmaikin, A.A. and Sunyaev, R.A. 1973, Astron. Zh., 50, 210

Ciolek, G.E., Mouschovias,T, Ch. 1995. ApJ, 454, 194

Goloviznin, V.M., Samarskii, A.A., Favorskii,A.P. 1976, " On artificial viscosity and stability of difference schemes of hydrodynamics. " , Preprint of the Institute of Applied Mathematics of the Russian Acad. Sci. No. 70, (in Russian)

Kulikovskii, A.G., Ljubimov, G.A. 1962, Magnetic Hydrodynamics, Fizmatlit, Moscow

Landay, L.D., Lifshitz, E.M. 1984, Electrodynamics of Continuous Media, 2nd ed.,Pergamon Press (Oxford)

Le Blank, L.M. and Wilson, J.R. 1970, ApJ, 161, 541

Moschovias, T., Ch., Paleologou, E.,V. 1979. ApJ, 230, 204

Moschovias, T., Ch., Paleologou, E.,V. 1980. ApJ, 237, 877

Ohnishi, T. 1983, Tech. Rep. Inst. At. En. Kyoto Univ., No.198

Osherovich, V.A., Tzur, I, Gliner, E.B. 1984, ApJ, 284, 412

Samarskii, A.A., Popov, Ju.P., 1992, Difference Methods for the Solution of Problems of Gas Dynamics. Moscow, Nauka, (in Russian)

Tomisaka, K. 1998. ApJ, 502, L163